J. Shanghai Jiao Tong Univ. (Sci.), 2018, 23(1): 175-181
https://doi.org/10.1007/s12204-018-1923-z

Numerical Investigation of Ultrasonic Guided Wave Dynamics in Piezoelectric Composite Plates for Establishing Structural Self-Sensing

WANG Junzhen (王军振), *SHEN Yanfeng** (申岩峰)
(University of Michigan - Shanghai Jiao Tong University Joint Institute,
Shanghai Jiao Tong University, Shanghai 200240, China)

Abstract: This article presents a numerical investigation of guided wave generation, propagation, interaction with damage, and reception in piezoelectric composite plates for the purpose of establishing structural self-awareness. This approach employs piezoelectric composite materials as both load bearing structure and sensing elements. Finite element modal analysis of a plate cell with Bloch-Floquet boundary condition (BFBC) is performed to understand the wave propagation characteristics in piezoelectric composite plates. A comparative study is carried out between a standard composite plate and a piezoelectric composite plate to highlight the influence of piezoelectricity on guided wave dispersion relations. Subsequently, a transient dynamic coupled-field finite element model is constructed to simulate the procedure of guided wave generation, propagation, interaction with damage, and reception in a piezoelectric composite plate. Active sensing array is designed to capture the structural response containing the damage information. Three engineering scenarios, including a pristine case, a one-damage-location case and a two-damage-location case, are considered to demonstrate the ultrasonic sensing capability of the piezoelectric composite system. Finally, time-reversal method is utilized to locate and image the damage zones. This research shows that piezoelectric composite material possesses great potential to establish structural self-awareness, if it serves both as the load bearing and structural sensing components.
Key words: piezoelectric composite, guided wave, time-reversal method, structural self-awareness
CLC number: O 313.7 **Document code:** A

0 Introduction

Piezoelectric materials can be made into both actuation and sensing device due to their inverse and direct piezoelectric properties. For example, piezoelectric wafer active sensors (PWASs) have been widely adopted as enablers for generating and receiving ultrasonic guided waves[1]. Besides, composite materials have been increasingly used in mechanical and aerospace structural design, serving as load bearing components with their superb strength, lightweight characteristics. Research efforts have been exerted on establishing structural self-awareness by introducing sensing elements into composite materials. Minakuchi and Takeda[2] implemented fiber optic sensors in aerospace composite structures for impact damage detection. Krishnamurthy et al.[3] embedded magnetostrictive particle layers in composite laminates and achieved delamination detection. To foster in-situ ultrasonic inspection of composites, researchers designed the intelligent composites with embedded piezoelectric sensors to establish the life-cycle health management capability. However, such an embedding practice would inevitably cause stress concentration in the materials and may eventually incubate local cracks. Paget et al.[4] conducted experiments on the performance of embedded piezoceramic transducer in mechanically loaded composites, and the results showed a low survival rate of the sensors. Taking an alternative approach, researchers have also tried to manipulate material properties by adding functional components. Tallman et al.[5] used carbon nanofiber/polyurethane for the fabrication of nanocomposites and realized enhanced delamination detection and distributed strain sensing. Gallo and Thostenson[6] distributed carbon nanotubes in composites to build structural self-sensing capability and managed to monitor material micro cracks. Haghiashtiani and Greminger[7] utilized polyvinylidene fluoride (PVDF) as the composite matrix for integrated structural load sensing. Such piezoelectric composite material demonstrated promising sensing capability in low frequency mechanical tests.

This study investigates the potential of a PVDF matrix composite material for integrating both load

Received date: 2017-08-30
Foundation item: the National Natural Science Foundation of China (No. 51605284)
∗**E-mail:** yanfeng.shen@sjtu.edu.cn

bearing and structural sensing in ultrasonic range. While sustaining the loads, each location across the piezoelectric composite member can serve as an actuator and a sensor. At one location, a material point under electric excitation can generate ultrasonic mechanical response due to the inverse piezoelectric effect. This mechanical disturbance will propagate along the structure as guided waves, interact with possible damage/fatigue, carry damage information with them, and finally be picked up by the electrodes at the sensing locations due to the direct piezoelectric effect. Such guided wave generation and reception capability enables the piezoelectric composite materials to establish self-awareness through the ultrasonic guided wave interrogations.

1 Guided Wave Characteristics in Piezoelectric Composites

The introduction of piezoelectric effects through the polling procedure may substantially influence the guided wave characteristics in terms of dispersion relations in a composite plate. Finite element method (FEM) with Bloch-Floquet boundary condition (BFBC) is adopted to obtain the fundamental understanding of guided wave mechanism in piezoelectric composite plates. Such FEM technique has been widely used to model dynamic response of periodic structures. Large scale waveguides have been treated as the connection of subsections of periodic components for the solution of dispersion curves and mode shapes[8]. Similarly, the piezoelectric composite plate can be treated as the assembly of unit cells of piezoelectric cubes. The piezoelectric effects enter the solution via the coupled field analysis.

Figure 1 presents the unit finite element cell with BFBC for a piezoelectric composite plate. The BFBC imposes constrains on the degrees of freedom (DoFs), implying phase delays between the unit cell boundaries. In Fig. 1, $U_{\text{in}} = \tilde{U}\mathrm{e}^{-\mathrm{i}\omega t}$ represents a harmonic oscillation, where t is time and $\tilde{U}$ is displacement; the outflowing wave displacements are $U_{\text{out2}} = U_{\text{in}}\mathrm{e}^{\mathrm{i}\xi_x a_x}$, $U_{\text{out3}} = U_{\text{in}}\mathrm{e}^{\mathrm{i}(\xi_x a_x + \xi_y a_y)}$ and $U_{\text{out4}} = U_{\text{in}}\mathrm{e}^{\mathrm{i}\xi_y a_y}$; ξ_x and ξ_y respectively represent the wavenumbers in the x and y directions, defining a corresponding wavelength at the angular frequency ω; a_x and a_y are the unit cell dimensions, and they usually take very small values, 0.1 mm for the current analysis, to accurately capture short wavelength ultrasonic waves. The solving scheme sweeps through the wavenumber domain. At each wavenumber, corresponding to a certain wavelength, the only unknown terms in the dynamic equation system are the frequencies. The phase relationships between the incidence wave displacement U_{in} and the outflowing wave displacements U_{out} at the boundaries are governed and constrained by the BFBC. Thus, the target problem retrieves to the conventional modal analysis, where the eigenvalues are the frequencies of the wave modes possessing the same defined wavelength and the eigenvectors represent their mode shapes. The physical interpretation of the solution mechanism can be perceived from the nature of guided waves: cross-sectional mechanical resonance propagating in the normal direction. It should be noted that the BFBC is applied on all the vertical boundary nodes. In addition to the corner nodes, if intermediate boundary nodes exist, they need to be compatible with the corresponding counter facing nodes, i.e., the counter facing nodes at $X = 0$ and $X = a_x$ should possess a phase difference of $\mathrm{e}^{\mathrm{i}\xi_x a_x}$. It should also be noted that, for the modeling of piezoelectric effects with coupled field analysis, the BFBC applies not only to displacement DoFs but also to voltage DoFs.

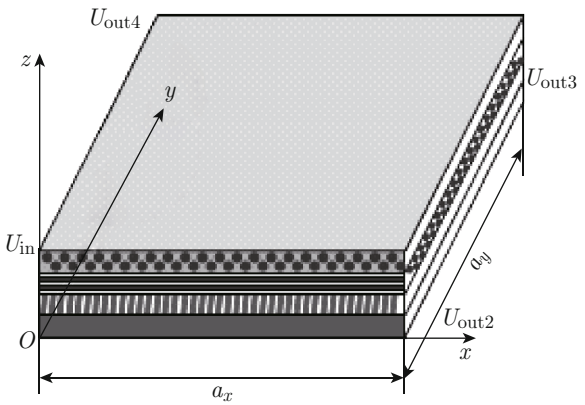

Fig. 1 Unit finite element cell with BFBC for the computation of guided wave dispersion and mode shapes in a piezoelectric composite plate

In order to better appreciate the influence of piezoelectricity on the dispersion relations of plate guided waves, numerical investigation on a glass fiber PVDF matrix composite plate is performed before and after the poling procedure. Before poling, the piezoelectric constants of the material are set to zero, while they take non-zero values after poling. It should be noted that the detailed material stiffness matrix and piezoelectric constants need to be obtained from the experimental measurements. However, this study focuses more on the phenomenological aspect of the active sensing procedure. Systematic experiment efforts will be performed in a future study. For current stage, a quasi-isotropic composite material property is assumed. Figure 2 shows the dispersion relations obtained from the Bloch-Floquet FEM. The multimodal dispersive nature of guided wave is obviously illustrated. Figure 2(a) presents the frequency-phase velocity dispersion relations of a 2 mm thick composite plate before poling, while Fig. 2(b) plots the dispersion curves after the introduction of piezoelectric effects. It is apparent

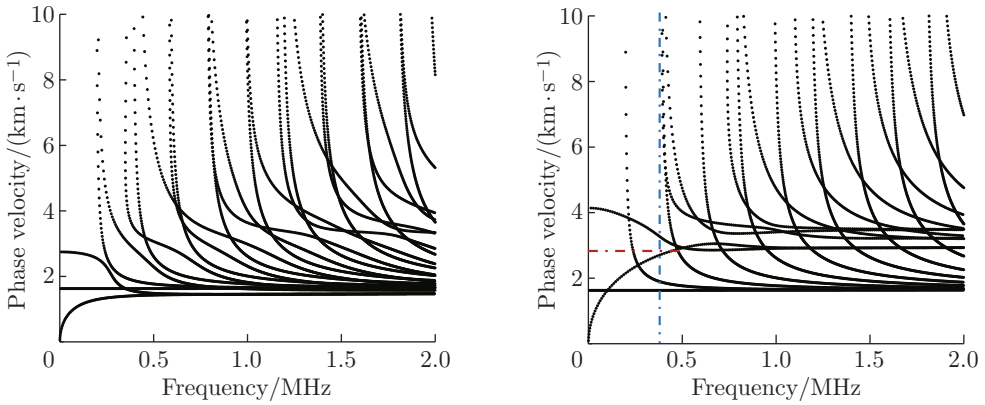

(a) Before poling (b) After poling and exhibiting piezoelectric effects

Fig. 2 Guided wave dispersion curve results for a 2 mm thick composite plate

that all the Lamb modes travel much faster with the coupling of mechanical and electrical quantities, and the cut-off frequencies shift to higher values. However, the shear horizontal modes are not influenced since the shear piezoelectric coupling coefficients are zero. The influence is especially obvious for the fundamental symmetric Lamb mode (denoted as S0). Before poling, the phase velocity is merely 2.748 km/s in the low frequency range, while it reaches 4.140 km/s with the piezoelectric effects. S0 also becomes much more dispersive. All the Lamb modes finally converge towards the surface guided Rayleigh waves, showing a much higher wave speed in the piezoelectric composite plate. For plate structures, with higher stiffness, phase velocity and cut-off frequency become higher. The classical piezoelectric constitutive equation can be found in Ref. [1]. The coupling effect induces a piezoelectric stress term. Thus with unit strain, the nominal stress value increases, rendering a higher apparent material stiffness, which may serve as the reason why all the Lamb modes possess higher phase velocities and cut-off frequencies. These distinctive dispersion variations are, after all, related to the piezoelectric constant values. The degree of influence needs to be further determined from experimental validations in a future work. For the initial stage of this study, a quasi-isotropic composite plate is considered, so the dispersion curves of all the directions are nearly the same.

2 Finite Element Modeling of Structural Sensing

On the basis of the comprehensive understanding of the guided wave features in the piezoelectric composite plate, the guided wave generation, propagation, interaction with damage, and reception will be further studied by a transient dynamic coupled field finite element model.

2.1 Finite Element Model and Sensing Array Design

Figure 3 shows the finite element model adopted for the simulation of guided wave active sensing in a 500 mm long, 500 mm wide, and 2 mm thick piezoelectric composite plate. Commercial finite element package ANSYS is used to conduct the simulation task. SOLID5 coupled field element is deployed to discretize the simulation domain. Extended region of absorbing layers with increasing damping (ALID) is implemented through surrounding the plate to eliminate the boundary reflections as well as to minimize the model size. Thus, the computation of wave propagation in infinitely large plates can be achieved with a finite size model. In wave dynamic simulations, there is always a dilemma on the mesh size. A suitable mesh size should be small enough to ensure accuracy and sufficiently large to minimize computational burden. So a careful

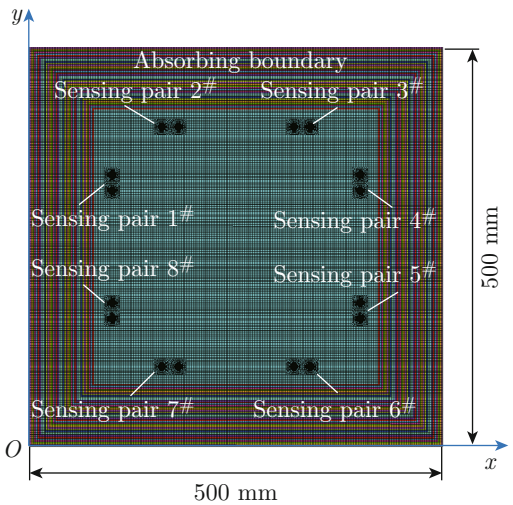

Fig. 3 Full-scale finite element model with eight sensing pairs

convergence study is conducted, as shown in Fig. 4. The root-mean-square (RMS) errors of the voltage response at the sensing electrode between the consecutive test meshing sizes are plotted. It shows that a mesh size of 10 elements per centimeter can satisfy both accuracy and efficiency requirements. Thus, the element size in the FEM model is selected as 1 mm × 1 mm × 0.5 mm. The piezoelectric composite material is used as both the structural and sensing components. Consequently, only surface bonded electrodes are needed at the designated actuation and sensing locations. In this study, a total number of eight sensing pairs are used in the sensing array design. Each sensing pair is comprised of one actuation electrode and one sensing electrode. The electrodes take the circular shape with a diameter of 10 mm. The actuation and sensing electrodes are placed 20 mm apart, forming the pulse-echo active sensing mode. The rational for such an array design aims to better identify the wave packets scattered from the damage. Guided waves generated by the actuation electrode reach the sensing location right after their emission as a direct incident wave packet. Then, they propagate along the plate structure, are scattered at the damage sites, and finally arrive at the sensing electrode as echo wave signals. Thus, ideally, after the direct incident wave packet, the rest of the waves are all from damage reflections. For case study, three engineering scenarios were considered: a pristine case, a one-damage-location case and a two-damage-location case. Without loss of generality, the damage for the one-damage-location case is at (290, 290) mm, and another damage at (170, 210) mm is additionally introduced for the two-damage-location case. These 2 cm by 2 cm through-thickness square damage zones are modeled via reducing the material stiffness by 90% within the damage areas.

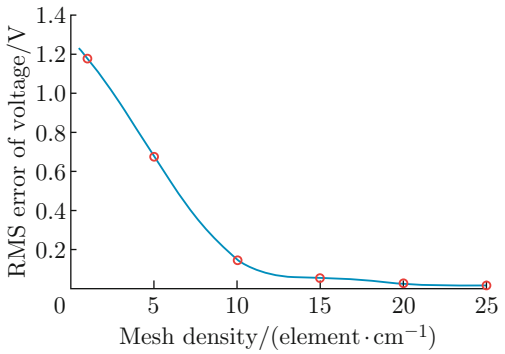

Fig. 4 Convergence study of mesh size in the finite element model

2.2 Finite Element Simulation Results for Guided Wave Active Sensing

Figure 5 shows the snapshots of the stress wave field as well as the representative sensing signals from the sensing pair 3#. Only single S0 wave mode is excited, which is quite different from conventional PWAS generated multimodal guided waves containing both S0 and A0 components. The excitability of guided wave modes depends on whether the excitation profile couples well with a certain mode shape. The reason behind single S0 mode excitation lies in the fact that the material

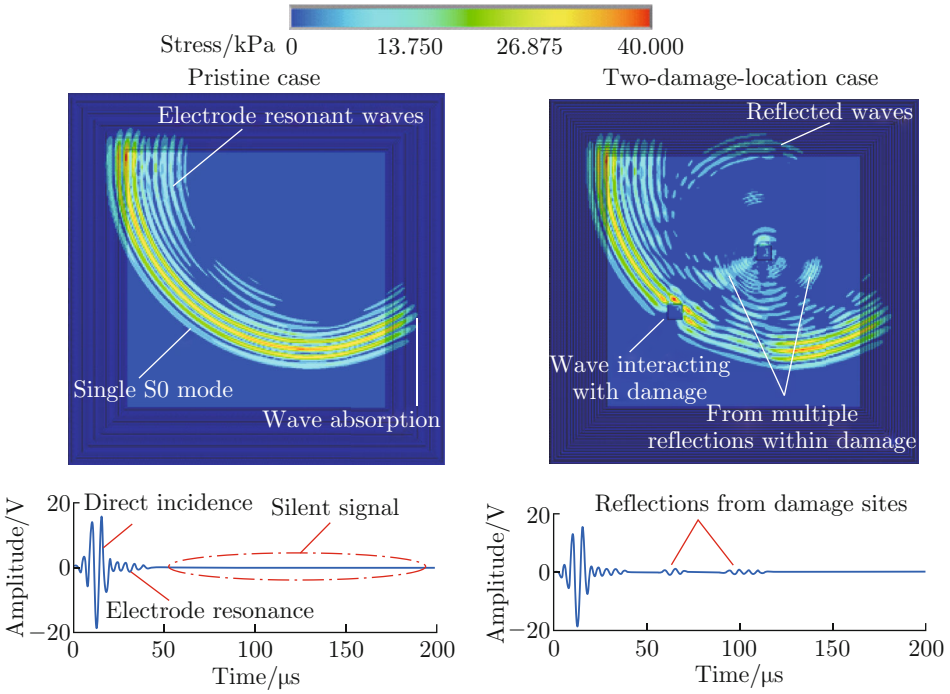

Fig. 5 The wave propagation snapshots and the sensing pair 3# signals in the piezoelectric composite plate

properties of the plate are symmetric with respect to the mid-plane, while the electric field is uniform cross the thickness. Such symmetric material layup and uniform electric field only induce symmetric deformation about the mid-plane, which couples well with the symmetric Lamb mode shapes rather than the anti-symmetric ones. Thus, the benefit of using piezoelectric composite plate as both structural and sensing members is that the complexity of sensing signals may be substantially reduced. Effective wave absorption at the ALID boundary can be noticed. Between the actuation and sensing electrodes, electromechanical resonances causing subtle sequential waves are observed. In the two-damage-location case, scattered waves from the damage can be clearly identified. Subtle wave packets are also found due to the multiple reflections within the damage zone. In the active sensing signals, for pristine case, only direct incident wave packet and electrode resonant waves are present in the beginning and silent signal follows. On the other hand, in the two-damage-location case, in addition to the incident wave and electrode resonant waves, two obvious echo wave packets appear from the reflections at the two damage locations. Signals from other sensing pairs resemble such situation and are not shown in details in this paper.

3 Time Reversal Method for Damage Imaging

In order to achieve high-quality structural sensing, damage localization and imaging techniques are employed, among which time reversal method has been extensively investigated and developed towards its mature stage[9-11]. Some recent progress on guided wave based damage imaging can be further found in Refs. [12-13]. Thus, the time reversal imaging algorithm is used to construct active sensing images.

The time reversal method virtually performs back propagation of the time reversed wave signal into the medium. Due to the reciprocity of the linear ultrasonic system, guided waves will trace back and focus on the wave sources. Scattering waves from damage are considered as a secondary wave source. The raw sensing signals are processed with window function to eliminate the influence from the direct incident wave packet. Then, the signals are further enveloped to represent the wave packet energy propagation and focusing phenomena. This signal processing procedure is presented in Fig. 6.

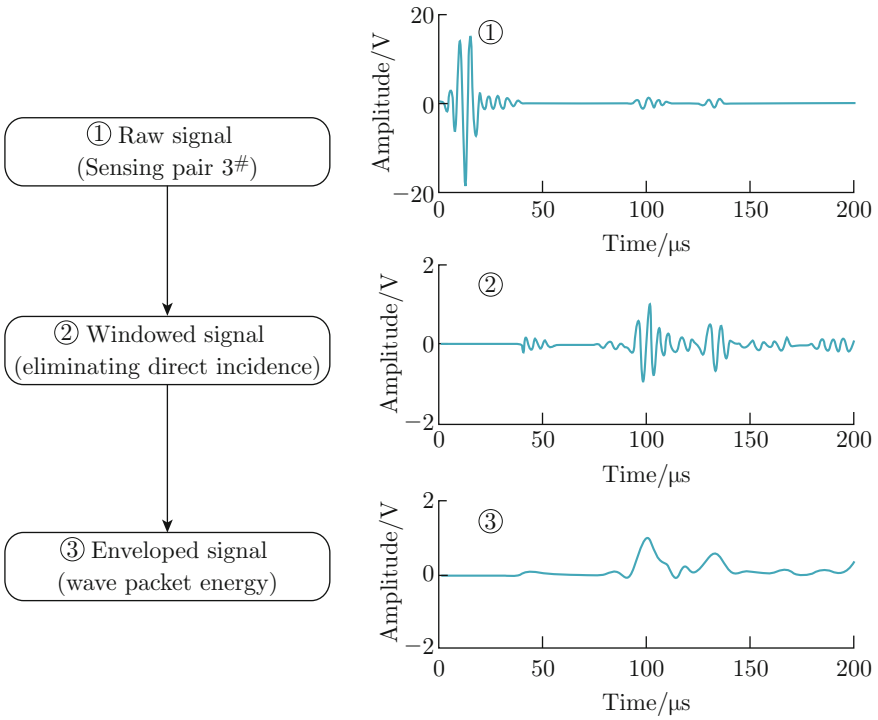

Fig. 6 Signals processed with window function and envelope curves

The "addition" imaging algorithm of time reversal method to compute the pixel value $S(i,j)$ at the location (i,j) is given by

$$S(i,j)=\sum_{m=1}^{N} A_m V_m(t_{mij}), \tag{1}$$

$$A_m = 10/\max(V_m),$$
$$t_{mij} = [R_m^{\mathrm{a}}(i,j) + R_m^{\mathrm{s}}(i,j)]/c_{\mathrm{g}},$$

where A_m is the unifying weighting function; $V_m(t_{mij})$ represents the time domain sensing signal after the windowing and enveloping procedure; t_{mij} stands for the

time elapse of wave propagation from the actuator to the pixel location (i, j) and back to the sensor; the subscript m represents the sensing pair m; N represents the maximum number of sensing pairs; R_m^{a} and R_m^{s} are the distances from the actuator to the pixel location and from the pixel location to the sensor, respectively; $c_{\mathrm{g}} = 3.439\,\mathrm{km/s}$ is the group velocity of S0 mode at 200 kHz obtained from the dispersion relations. If the time elapse exceeds the maximum simulation time, the pixel value of the location is set to zero. 500 pixel locations are equally spaced on each side, so it means totally 250 000 pixel locations for imaging. Similarly, in order to highlight the pixel value of each pixel location, the "multiplication" algorithm can be written as

$$S(i,j) = \prod_{m=1}^{N} A_m V_m(t_{mij}). \tag{2}$$

Figure 7 presents the time reversal imaging results for three situations (the first row: pristine case; the second row: one-damage-location case; the third row: two-damage-location case). Remarkable accuracy is found for damage localization and imaging.

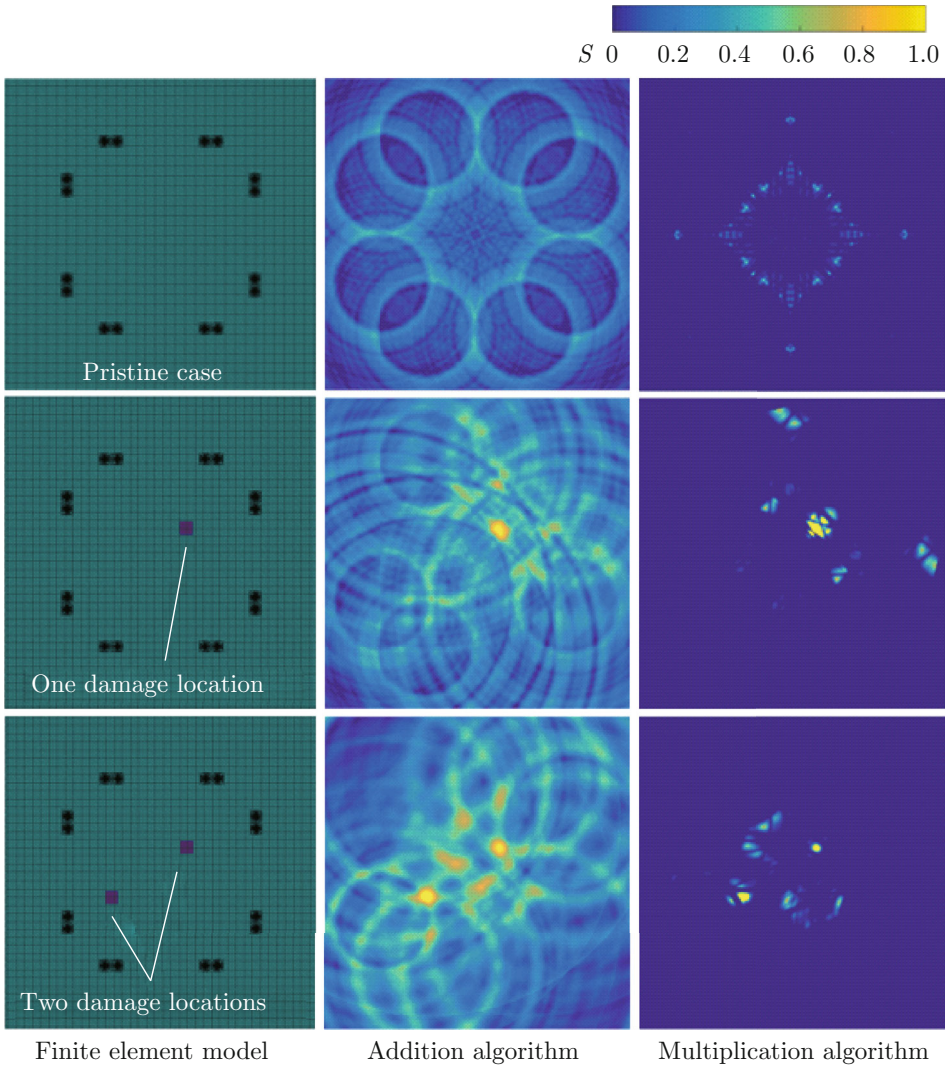

Fig. 7 Time reversal results for damage localization and imaging

4 Conclusion

This article presents a numerical investigation of piezoelectric composites for establishing structural self-sensing capability. A Bloch-Floquet FEM procedure is deployed to obtain the dispersion relations and demonstrate the influence from piezoelectricity on guided wave propagation. Transient dynamic coupled field finite element modeling is performed to simulate guided wave generation, propagation, interaction with damage, and reception. It is found that signal S0 mode is generated, which may substantially reduce the signal complexity. A time reversal method is utilized to locate the damage. The imaging results show remarkable

agreement with the physical damage locations. This research shows that piezoelectric composite material possesses great potential to establish structural self-awareness.

References

[1] GIURGIUTIU V. Structural health monitoring with piezoelectric wafer active sensors [M]. Amsterdam: Academic Press, 2007.

[2] MINAKUCHI S, TAKEDA N. Recent advancement in optical fiber sensing for aerospace composite structures [J]. *Photonic Sensors*, 2013, **3**(4): 345-354.

[3] KRISHNAMURTHY A V, ANJANAPPA M, WANG Z, et al. Sensing of delaminations in composite laminates using embedded magnetostrictive particle layers [J]. *Journal of Intelligent Material Systems and Structures*, 1999, **10**: 825-835.

[4] PAGET C A, LEVIN K, DELEBARRE C. Actuation performance of embedded piezoceramic transducer in mechanically loaded composites [J]. *Smart Materials and Structures*, 2002, **11**(6): 886-891.

[5] TALLMAN T N, GUNGOR S, WANG K W, et al. Tactile imaging and distributed strain sensing in highly flexible carbon nanofiber/polyurethane nanocomposites [J]. *Carbon*, 2015, **95**: 485-493.

[6] GALLO G J, THOSTENSON E T. Electrical characterization and modeling of carbon nanotube and carbon fiber self-sensing composites for enhanced sensing of microcracks [J]. *Materials Today Communications*, 2015, **3**: 17-26.

[7] HAGHIASHTIANI G, GREMINGER M A. Fabrication, polarization, and characterization of PVDF matrix composites for integrated structural load sensing [J]. *Smart Materials and Structures*, 2015, **24**(4): 045038.

[8] ÅBERG M, GUDMUNDSON P. The usage of standard finite element codes for computation of dispersion relations in materials with periodic microstructure [J]. *The Journal of the Acoustical Society of America*, 1997, **102**(4): 2007-2013.

[9] QIU L, YUAN S F, ZHANG X Y, et al. A time reversal focusing based impact imaging method and its evaluation on complex composite structures [J]. *Smart Materials and Structures*, 2011, **20**(10): 105014.

[10] QIU L, LIU M L, QING X L, et al. A quantitative multidamage monitoring method for large-scale complex composite [J]. *Structural Health Monitoring*, 2013, **12**(3): 183-196.

[11] QIU L, LIU B, YUAN S F, et al. Impact imaging of aircraft composite structure based on a model-independent spatial-wavenumber filter [J]. *Ultrasonics*, 2016, **64**: 10-24.

[12] YU L Y, TIAN Z H, ZIEHL P, et al. Crack detection and evaluation in grout structures with passive/active methods [J]. *Journal of Materials in Civil Engineering*, 2016, **28**(4): 04015168.

[13] TIAN Z H, YU L Y, LECKEY C. Rapid guided wave delamination detection and quantification in composites using global-local sensing [J]. *Smart Materials and Structures*, 2016, **25**(8): 085042.